RSC Advances

PAPER

View Article Online
View Journal | View Issue

Cite this: *RSC Adv.*, 2019, **9**, 1491

Co-culture of the fungus *Fusarium tricinctum* with *Streptomyces lividans* induces production of cryptic naphthoquinone dimers†

Mariam Moussa,[a] Weaam Ebrahim,[ab] Michele Bonus,[c] Holger Gohlke,[cd] Attila Mándi,[e] Tibor Kurtán,[e] Rudolf Hartmann,[f] Rainer Kalscheuer,[a] Wenhan Lin,[g] Zhen Liu *[a] and Peter Proksch*[a]

Co-cultivation of the endophytic fungus *Fusarium tricinctum* with *Streptomyces lividans* on solid rice medium led to the production of four new naphthoquinone dimers, fusatricinones A–D (**1–4**), and a new lateropyrone derivative, dihydrolateropyrone (**5**), that were not detected in axenic fungal controls. In addition, four known cryptic compounds, zearalenone (**7**), (−)-citreoisocoumarin (**8**), macrocarpon C (**9**) and 7-hydroxy-2-(2-hydroxypropyl)-5-methylchromone (**10**), that were likewise undetectable in extracts from fungal controls, were obtained from the co-culture extracts. The known antibiotically active compound lateropyrone (**6**), the depsipeptides enniatins B (**11**), B1 (**12**) and A1 (**13**), and the lipopeptide fusaristatin A (**14**), that were present in axenic fungal controls and in co-culture extracts, were upregulated in the latter. The structures of the new compounds were elucidated by 1D and 2D NMR spectra as well as by HRESIMS data. The relative and absolute configuration of dihydrolateropyrone (**5**) was elucidated by TDDFT-ECD calculations.

Received 1st November 2018
Accepted 2nd January 2019

DOI: 10.1039/c8ra09067j

rsc.li/rsc-advances

Introduction

Cultivating microorganisms under axenic laboratory conditions fails to resemble the natural environment where these microbes are subjected to intense microbial competition. Therefore naturally occurring stimulants and signal molecules that are involved in chemical communication and antagonism between different microbes are absent, which may result in silencing biosynthetic gene clusters and in simplified metabolite patterns.[1,2] The endophytic fungus *Fusarium tricinctum* has already been well investigated with regard to its natural products.[3–5] Applying the OSMAC (One Strain MAny Compounds) approach on cultures of this fungus resulted in the accumulation of new bioactive secondary metabolites such as fusarielin congeners[3] and in an enhanced production of enniatin derivatives.[4] Enniatins are known for their anti-cancer, anti-HIV as well as for their antibacterial activities.[5–7] Enniatins A–C (named fusafungin) were even once available on the drug-market as a local antibiotic for the treatment of respiratory infections. However, due to undesired side effects this approval has meanwhile been withdrawn.[8]

Previous co-cultivation experiments with *F. tricinctum* focused on *Bacillus subtilis* as a prokaryotic antagonist. Co-culture of both microbes on solid rice medium resulted in a dramatically enhanced (up to 80-fold) accumulation of several fungal metabolites including enniatins, the polyketide lateropyrone and the lipopeptide fusaristatin A.[5] Whereas all of the latter compounds were also observed in axenic fungal controls (albeit at much lower concentrations), the co-cultures yielded several additional cryptic metabolites such as macrocarpon C, (−)-citreoisocoumarinol, and (−)-citreoisocoumarin.[5]

Previous experiments also indicated that fungi when co-cultured with different bacteria respond through accumulation of different cryptic metabolites. For example, treatment of the fungus *Chaetomium* sp. with autoclaved cultures of *Pseudomonas aeruginosa* yielded new butenolide derivatives,[9] whereas co-culture of the same fungus with live cultures of *B. subtilis* yielded new shikimic acid derivatives.[10]

[a]*Institute of Pharmaceutical Biology and Biotechnology, Heinrich-Heine-Universität Düsseldorf, Universitätsstrasse 1, 40225 Düsseldorf, Germany. E-mail: zhenfeizi0@sina.com; proksch@uni-duesseldorf.de*

[b]*Department of Pharmacognosy, Faculty of Pharmacy, Mansoura University, Mansoura 35516, Egypt*

[c]*Institute of Pharmaceutical and Medicinal Chemistry, Heinrich-Heine-Universität Düsseldorf, Universitätsstrasse 1, 40225 Düsseldorf, Germany*

[d]*John von Neumann Institute for Computing (NIC), Jülich Supercomputing Centre (JSC), Institute for Complex Systems – Structural Biochemistry (ICS-6), Forschungszentrum Jülich GmbH, Wilhelm-Johnen-Straße, 52425 Jülich, Germany*

[e]*Department of Organic Chemistry, University of Debrecen, Egyetem tér 1, Debrecen 4032, Hungary*

[f]*Institute of Complex Systems – Structural Biochemistry, Forschungszentrum Jülich GmbH, Wilhelm-Johnen-Straße, 52428 Jülich, Germany*

[g]*State Key Laboratory of Natural and Biomimetic Drugs, Peking University, Beijing 100191, China*

† Electronic supplementary information (ESI) available: MS, 1D and 2D NMR spectra of compounds **1–5**. See DOI: 10.1039/c8ra09067j

Here we have studied the influence of *Streptomyces lividans* on accumulation of natural products by *F. tricinctum*. *S. lividans* is known both as a plant-endophyte[11] or as a soil-bacterium.[12,13] Co-cultivation of *F. tricinctum* and *S. lividans* resulted in the accumulation of several new compounds, the dimeric naphthoquinones (**1–4**) and dihydrolateropyrone (**5**), that were not detected in axenic fungal controls (Fig. 1). In addition, several known metabolites such as enniatin derivatives (**11–13**) showed an enhanced accumulation in the co-cultures. Structure elucidation of the new compounds by one- and two-dimensional NMR, HRMS, ECD and quantum chemical calculations is discussed.

Results and discussion

The EtOAc extracts of both axenic fungal cultures and co-cultures resulting from mixed fermentation of *F. tricinctum* and *S. lividans* on solid rice medium were analyzed by HPLC. When fermented axenically on solid rice medium containing liquid YM medium, the fungus accumulates a complex pattern of bioactive metabolites consisting of several enniatines (**11–13**), polyketides (*e.g.* lateropyrone, **6**) and lipopeptides (*e.g.* fusaristatin A, **14**). By comparison of the chromatograms, a dramatic shift in the metabolic profile of the co-cultures compared to the axenic fungal or bacterial controls was obvious. These changes are presented in Table 1 indicating a pronounced (up to 12-fold) upregulation of constitutively present metabolites and induction of several cryptic compounds. Chromatographic workup of the co-culture extracts yielded five new compounds (**1–5**) that were not detected in either fungal or bacterial axenic controls.

Table 1 Yield of induced metabolites per flask of co-culture of *F. tricinctum* and *S. lividans* ($n = 6$) *vs.* axenic controls of *F. tricinctum* ($n = 4$)

Compound	Fungal control (mg)	Co-culture (mg)	Increase (fold)
1	n.d.[a]	7.67 ± 0.1	
2	n.d.	+[c]	
3	n.d.	+	
4	n.d.	+	
5	n.d.	+	
6	1.3 ± n.a.[b]	17.0 ± 0.8	12.5
7	n.d.	+	
8	n.d.	12.5 ± 10.4	
9	n.d.	+	
10	n.d.	+	
11	250.7 ± 50.2	868.9 ± 38.0	3.5
12	203.8 ± 31.8	459.5 ± 25.3	2.3
13	47.6 ± 32.3	95.7 ± 8.9	2.0
14	175.2 ± 54.0	294.8 ± 11.4	1.7

[a] n.d. = not detected. [b] n.a. = not available. [c] Isolated but not detected in all crude extracts.

Compound **1** exhibited distinct UV absorption maxima at λ_{max} 320, 278 and 223 nm. The HRESIMS data of **1** established the molecular formula $C_{31}H_{24}O_{16}$, indicating twenty degrees of unsaturation. The ^{1}H NMR spectrum of **1** (Table 2) showed fewer signals in comparison to the molecular formula, suggesting the possible dimeric nature of **1**. These signals included two singlet aromatic protons at δ_H 7.17 (H-8/8′), two singlet methyl groups at δ_H 1.88 (Me-14) and 1.86 (Me-14′), two singlet methylene groups at δ_H 3.08 (H_2-12′) and 3.03 (H_2-12), in addition to three methoxy groups at δ_H 4.10 (Me-15/15′) and 3.68 (Me-16′). In the HMBC spectrum of **1**, ^3J-HMBC correlations

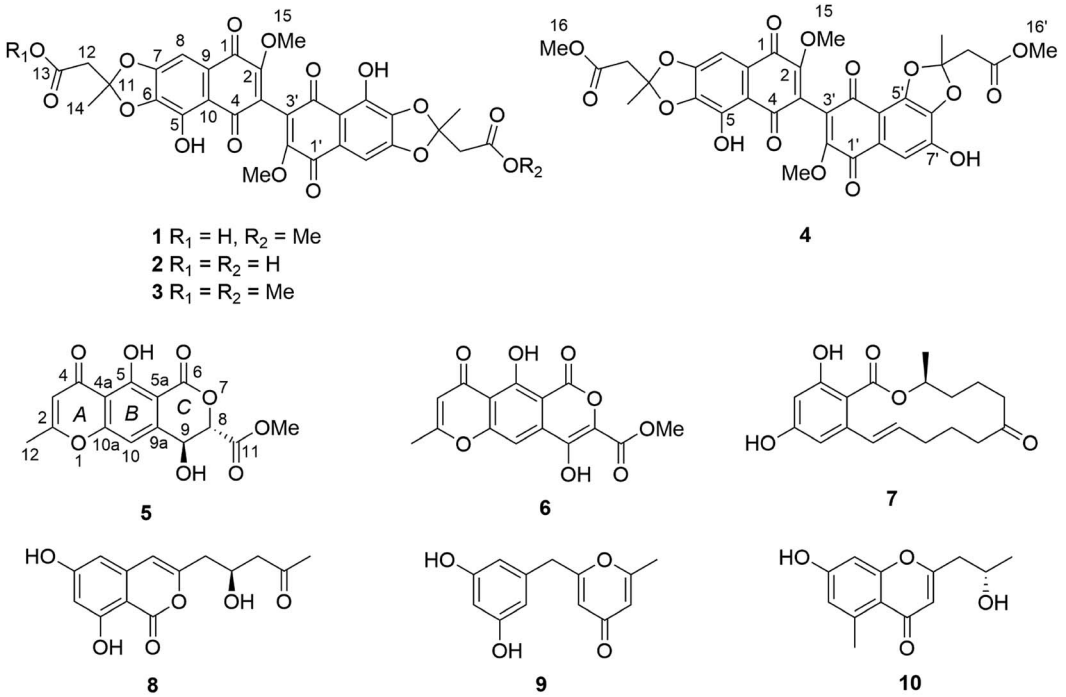

Fig. 1 Structures of compounds **1–10**.

Table 2 NMR data of compound **1**[a]

	1a		1b	
Position	δ_C, type	δ_H (J in Hz)	δ_C, type	δ_H (J in Hz)
1/1′	179.5, C		179.5, C	
2/2′	159.0, C		159.0, C	
3/3′	121.2, C		121.2, C	
4/4′	188.3, C		188.3, C	
5/5′	145.4, C		145.4, C	
6/6′	139.8, C		139.8, C	
7/7′	152.8, C		152.8, C	
8/8′	102.5, CH	7.17, s	102.5, CH	7.17, s
9/9′	127.2, C		127.2, C	
10/10′	112.5, C		112.5, C	
11	120.4, C		120.4, C	
12	43.5, CH_2	3.03, s	43.5, CH_2	3.03, s
13	169.9, C		169.9, C	
14	24.8, CH_3	1.88, s	24.8, CH_3	1.88, s
15	61.6, CH_3	4.10, s	61.6, CH_3	4.09, s
11′	120.1, C		120.1, C	
12′	43.3, CH_2	3.08, s	43.3, CH_2	3.08, s
13′	168.5, C		168.5, C	
14′	25.1, CH_3	1.86, s	25.1, CH_3	1.86, s
15′	61.6, CH_3	4.09, s	61.6, CH_3	4.09, s
16′	52.5, CH_3	3.68, s	52.5, CH_3	3.68, s

[a] Measured in $CDCl_3$–CD_3OD (2 : 1) (^1H at 600 MHz and ^{13}C at 150 MHz).

from H-8 to C-1 (δ_C 179.5), C-6 (δ_C 139.8) and C-10 (δ_C 112.5), and from Me-15 to C-2 (δ_C 159.0) as well as weak ^2J-HMBC correlations from H-8 to C-7 (δ_C 152.8) and C-9 (δ_C 127.2) were observed. In addition, H-8 showed long range ^4J-HMBC correlations to C-2, C-4 (δ_C 188.3) and C-5 (δ_C 145.4), while Me-15 exhibited long range HMBC correlations to C-1, C-3 (δ_C 121.2), C-4 and C-9. Furthermore, when the spectra were recorded in $CDCl_3$, an additional signal at δ_H 12.04 assigned for OH-5 was detected which showed HMBC correlations to C-5, C-6 and C-10. These findings confirmed the presence of a dimeric substituted naphthoquinone core structure of **1** through a C-3/3′ linkage (Fig. 1). A methoxy and a hydroxy group were located at C-2/2′ and C-5/5′, respectively. Apart from these, the HMBC correlations from Me-14 to C-11 (δ_C 120.4) and C-12 (δ_C 43.5), and from H_2-12 to C-11, C-13 (δ_C 169.9) and C-14 together with the HMBC correlations from Me-14′ to C-11′ (δ_C 120.1) and C-12′ (δ_C 43.3), from H_2-12′ to C-11′, C-13′ (δ_C 168.5) and C-14′, and from Me-16′ to C-13′, indicated the presence of two side chains from C-14 to C-13 and from C-14′ to C-16′ as shown. Based on the molecular formula and the chemical shifts of **1**, these two side chains are connected to the core structure through two acetonide rings between C-6/6′, C-7/7′ and C-11/11′. Thus, the structure of **1**, to which the trivial name fusatricinone A is given, was established as shown.

The UV pattern and NMR data of compound **2** (Table 3) resembled those of **1**, suggesting their structural similarity. The molecular formula $C_{30}H_{22}O_{16}$ of **2** was determined by the HRESIMS data, differing from that of **1** by the loss of 14 amu, which was due to the absence of the carboxymethyl group of **1** as shown by comparison of the 1D and 2D NMR spectra of both

Table 3 NMR data of compound **2**[a]

	2a		2b	
Position	δ_C,[b] type	δ_H (J in Hz)	δ_C,[b] type	δ_H (J in Hz)
1/1′	179.1, C		179.1, C	
2/2′	158.6, C		158.6, C	
3/3′	n.d.[c]		n.d.[c]	
4/4′	188.3, C		188.3, C	
5/5′	145.5, C		145.5, C	
6/6′	139.1, C		139.1, C	
7/7′	152.1, C		152.1, C	
8/8′	102.0, CH	7.21, s	102.0, CH	7.20, s
9/9′	127.1, C		127.1, C	
10/10′	112.2, C		112.2, C	
11/11′	119.2, C		119.2, C	
12/12′	42.9, CH_2	3.12, s	42.9, CH_2	3.10, s
13/13′	171.4, C		171.4, C	
14/14′	24.6, CH_3	1.91, s	24.6, CH_3	1.88, s
15/15′	61.2, CH_3	4.13, s	61.2, CH_3	4.12, s
OH-5/OH-5′		12.06, s	12.06, s	

[a] Measured in $CDCl_3$ (^1H at 600 MHz and ^{13}C at 150 MHz). [b] Data were extracted from the HSQC and HMBC spectra. [c] n.d. = not detected.

compounds. In addition, the 1D NMR of **2** showed the same chemical shifts for related nuclei in both molecule halves, indicating that both molecule halves are constitutionally identical. Thus, **2** was identified as a new natural product and was given the trivial name fusatricinone B.

The molecular formula of compound **3** was determined as $C_{32}H_{26}O_{16}$ based on the HRESIMS data, differing from that of **1** by an additional 14 amu and implying the presence of an additional methyl group in **3**. The UV and NMR (Table 4) data of **3** were similar to those of **2** and likewise exhibited only one set of NMR signals, indicating methylation of both terminal

Table 4 NMR data of compound **3**[a]

	3a		3b	
Position	δ_C,[b] type	δ_H (J in Hz)	δ_C,[b] type	δ_H (J in Hz)
1/1′	179.3, C		179.3, C	
2/2′	158.7, C		158.7, C	
3/3′	n.d.[c]		n.d.[c]	
4/4′	n.d.[c]		n.d.[c]	
5/5′	145.4, C		145.4, C	
6/6′	139.3, C		139.3, C	
7/7′	152.6, C		152.6, C	
8/8′	102.0, CH	7.21, s	102.0, CH	7.21, s
9/9′	127.6, C		127.6, C	
10/10′	112.1, C		112.1, C	
11/11′	119.5, C		119.5, C	
12/12′	43.3, CH_2	3.07, s	43.3, CH_2	3.06, s
13/13′	167.6, C		167.6, C	
14/14′	24.7, CH_3	1.90, s	24.7, CH_3	1.89, s
15/15′	61.2, CH_3	4.13, s	61.2, CH_3	4.12, s
16/16′	52.0, CH_3	3.71, s	52.0, CH_3	3.71, s
OH-5/OH-5′		12.05, s		12.05, s

[a] Measured in $CDCl_3$ (^1H at 600 MHz and ^{13}C at 150 MHz). [b] Data were extracted from the HSQC and HMBC spectra. [c] n.d. = not detected.

carboxyl groups to form the respective methyl ester functions. This deduction was further confirmed by the HMBC correlation from Me-16/16′ (δ_H 3.71) to C-13/13′ (δ_C 167.6). The trivial name fusatricinone C was assigned to the new compound **3**.

Compound **4** had the same molecular formula as that of **3** ($C_{32}H_{26}O_{16}$) as established by HRESIMS. The UV spectrum was similar to those of compounds **1–3**, suggesting the presence of the same naphthoquinone core structure. Unlike **3**, however, the ^{1}H and ^{13}C NMR spectra of the monomers of **4** (Table 5) exhibited two sets of signals, one of which (from C-1 to C-16) showed the same pattern as that of the monomer in **3**. The second monomer of **4** showed signals accounting for the aromatic proton at δ_H 7.23 (H-8′) and a hydroxy group at δ_H 11.10 (OH-7′), which are key signals to determine the substitution pattern of the second monomer. The HMBC spectrum of **4** displayed correlations from H-8′ to C-6′ (δ_C 140.2), C-7′ (δ_C 144.3), C-10′ (δ_C 107.6) and C-1′ (δ_C 178.6), and from OH-7′ to C-6′, C-7′ and C-8′ (δ_C 111.4). In addition, a ROESY correlation between H-8′ and OH-7′ was observed. These data indicated that cyclisation of one acetonide moiety of **4** included the oxygens at the C-5′ and C-6′ positions. Thus, the structure of **4** was elucidated as shown and the trivial name fusatricinone D was assigned to this compound.

Table 5 NMR data of compound **4**[a]

	4a		**4b**	
Position	δ_C,[b] type	δ_H (J in Hz)	δ_C,[b] type	δ_H (J in Hz)
1	179.0, C		179.0, C	
2	158.5, C		158.5, C	
3	n.d.[c]		n.d.[c]	
4	n.d.[c]		n.d.[c]	
5	143.8, C		143.8, C	
6	139.3, C		139.3, C	
7	152.4, C		152.4, C	
8	101.1, CH	7.16, s	101.1, CH	7.16, s
9	n.d.[c]		n.d.[c]	
10	111.8, C		111.8, C	
11	120.0, C		120.0, C	
12	42.1, CH_2	3.29, s	42.1, CH_2	3.28, s
13	167.9, C		167.9, C	
14	24.2, CH_3	1.82, s	24.2, CH_3	1.81, s
15	60.4, CH_3	3.96, s	60.4, CH_3	3.95, s
16	52.0, CH_3	3.57, s	52.0, CH_3	3.56, s
OH-5		11.80, s		11.79, s
1′	178.6, C		178.6, C	
2′	157.8, C		157.8, C	
3′	n.d.[c]		n.d.[c]	
4′	n.d.[c]		n.d.[c]	
5′	n.d.[c]		n.d.[c]	
6′	140.2, C		140.2, C	
7′	144.3, C		144.3, C	
8′	111.4, CH	7.23, s	111.4, CH	7.23, s
9′	n.d.[c]		n.d.[c]	
10′	107.6, C		107.6, C	
11′	120.0, C		120.0, C	
12′	41.8, CH_2	3.24, s	41.8, CH_2	3.24, s
13′	167.9, C		167.9, C	
14′	24.6, CH_3	1.80, s	24.6, CH_3	1.80, s
15′	60.7, CH_3	4.01, s	60.7, CH_3	4.00, s
16′	52.0, CH_3	3.59, s	52.0, CH_3	3.59, s
OH-7′		11.10, s		11.10, s

[a] Measured in DMSO-d_6 (^{1}H at 600 MHz and ^{13}C at 150 MHz). [b] Data were extracted from the HSQC and HMBC spectra. [c] n.d. = not detected.

Compounds **1–4** were detected in the original fungal-bacterial co-culture crude EtOAc extract by LC-MS, indicating that they are true natural products and not formed through methylation during chromatographic workup.

The ^{1}H NMR data of dimeric naphthoquinone core structure of **1–3** were comparable to those of synthetic 3,3′-dimethoxy-8,8′-dihydroxy-2,2′-bi-1,4-naphthoquinone, which exhibited signals of methoxy groups at δ_H 4.15 and signals of hydroxy groups at δ_H 12.08.[14,15]

For the isolated dimeric naphthoquinones **1–4**, the 3/3′-biaryl linkage between monomers can lead to axial chirality if the rotational energy barrier is sufficiently high.[16] DFT quantum chemical calculations of the rotation energy barrier for the biaryl axis were performed to check the possibility of atropisomers or interconversion of R_a and S_a conformers, which yielded ~22 kcal mol^{-1} for the inversion (Fig. 2), indicating that the atropisomers interconvert with a half-life of ~1.7×10^3 s = ~28 min at 300 K.[17,18]

Compounds **1–4** gave baseline ECD spectra and zero specific rotation. Each monomer contains one chiral center (C-11 and C-11′), and there is a configurationally labile biaryl axis, which is expected to allow the interconversion of R_a and S_a conformers in solution. Provided that the monomers have identical absolute configuration for the central chirality elements, namely (11*R*,11′*R*) or (11*S*,11′*S*) absolute configuration, distinct ECD spectra would be expected for **1–4** as observed for biaryls with central chirality but low rotational energy barrier exemplified by dicerandrol B,[19] and versixanthone C.[20] Thus the baseline ECD curves suggest stereoisomeric mixtures of **1–4** containing either equimolar amounts of (11*R*,11′*R*) and (11*S*,11′*S*) stereoisomers or four stereoisomers with (11*R*,11′*R*), (11*S*,11′*S*), (11*S*,11′*R*), (11*R*,11′*S*) absolute configuration. If there is a mixture of two quasi-enantiomers [(11*R*,11′*R*) and (11*S*,11′*S*)], the duplication of NMR signals derives from the slowly interconverting R_a and S_a conformers, which represent rotational diastereomers (Fig. 3A). If there is a mixture of four stereoisomers or two racemates [(11*R*,11′*R*), (11*S*,11′*S*), (11*S*,11′*R*), (11*R*,11′*S*)], the duplication can be due to diastereomers that differ in the configuration of the central chirality elements [(11*S**,11′*S**) *versus* (11*S**,11′*R**)], but not due to stereoisomers with enantiomorphic molecule halves [(11*S*,11′*R*) *versus* (11*R*,11′*S*)] (Fig. 3B). However, it is more likely that the slowly interconverting R_a and S_a conformers with homomorphic molecule halves are distinguished by the NMR even in this case, and the remote central chirality elements do not result in duplication of NMR signals.

The related biaryl derivative xanthomegnin, which was isolated from several *Penicillium* and *Aspergillus* species and occurs naturally as a 1 : 1 mixture of atropisomers,[21] has the same naphthoquinone core structure as compounds **1–4** isolated in this study, but the condensed 1,3-dioxolane ring is replaced by a δ-lactone ring. The biogenetic precursor of xanthomegnin is (*R*)-semivioxanthin, and xanthomegnin has a distinct ECD spectrum allowing configurational assignment of analogues.[22]

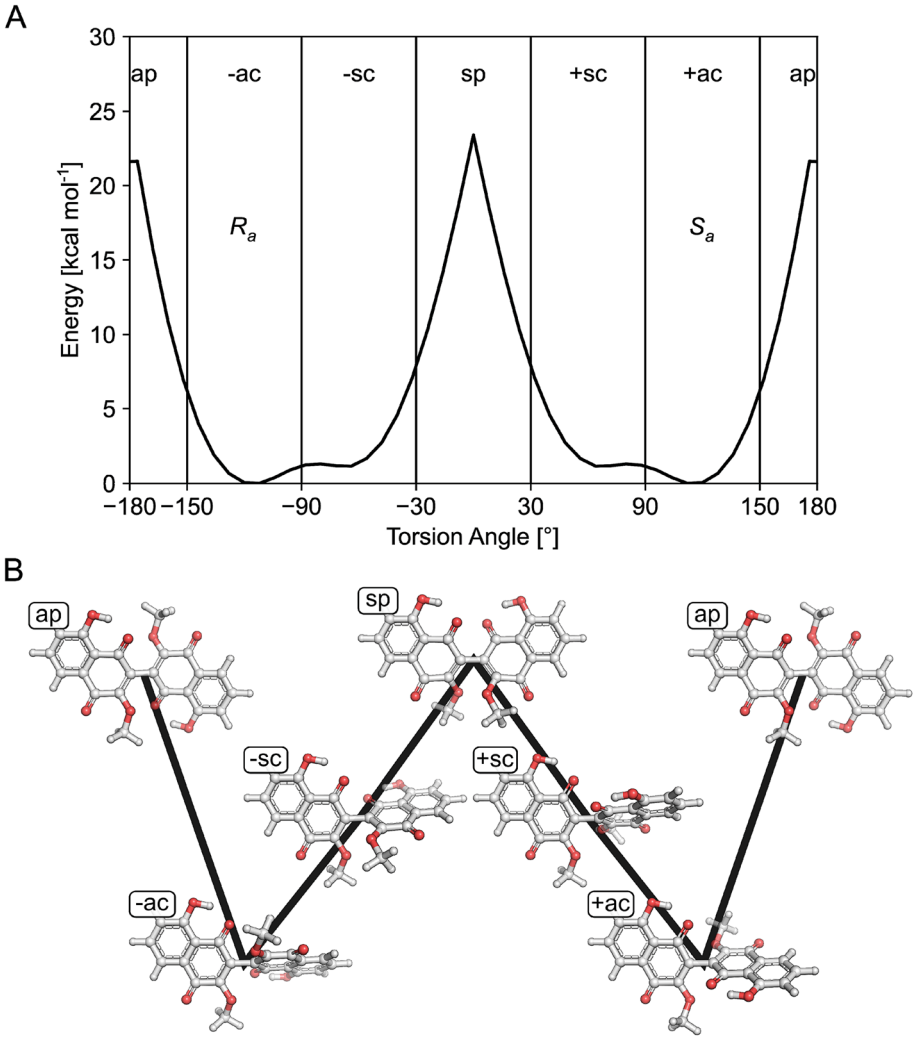

Fig. 2 Calculation of the height of the rotation barrier for compounds **1–4**. (A) Conformational energy profile obtained for the gas phase at the B3LYP/6-31G(d) level of theory for the rotation about the central biaryl bond in the model compound 8,8′-dihydroxy-3,3′-dimethoxy-2,2′-binaphthyl-1,1′,4,4′-tetrone. Vertical lines separate regions of values for the torsion angle that correspond to distinct conformations according to the Klyne–Prelog notation. The structures of the R_a and S_a atropisomers are assigned to the corresponding minimum-energy conformers in the anticlinal conformations. (B) Visualization of the distinct conformers according to the Klyne–Prelog notation. The height of the black line indicates the relative energy of the depicted conformer.

In the biosynthesis of xanthomegnin, the optically active monomers are formed first and are then dimerized by oxidative coupling.[23]

Compound **5** showed UV absorption maxima at 350, 263, 243 and 229 nm and had the molecular formula $C_{15}H_{12}O_8$ based on the HRESIMS data. Compound **5** contains two additional protons compared to the co-isolated structurally related known compound lateropyrone (**6**),[24] suggesting hydrogenation of the olefinic double bond of **6** at C-8 and 9, thus yielding **5**. This was also evident from the ^{1}H NMR spectrum of **5** (Table 6), which exhibited two aromatic protons at δ_H 6.36 (s, H-3) and 7.38 (s, H-10), two oxygenated methines at δ_H 4.92 (br s, H-9) and 6.04 (br s, H-8), an aromatic methyl group at δ_H 2.51 (s, Me-12) in addition to a methoxy group at δ_H 3.73 (s, OMe-11). The HMBC correlations from H-3 to C-2 (δ_C 170.9), C-4 (δ_C 184.4) and C-4a (δ_C 113.1), from Me-12 to C-2 and C-3, and from H-10 to C-10a (δ_C 158.1), C-9a (δ_C 125.6) and C-4a indicated the presence of the same rings A and B in **5**. However, the HMBC correlation from H-8 to C-6 (δ_C 168.6), C-11 (δ_C 170.6), C-9a (δ_C 125.6) and from H-9 to C-11 and C-9a confirmed the disappearance of the double bond of **6** in **5**.

Based on the small $^3J_{H\text{-}8,H\text{-}9}$ coupling constant value, a *cis* relative configuration of **5** was expected, and hence TDDFT-ECD calculations were performed on the arbitrarily chosen *cis*-(8*R*,9*S*) stereoisomer.[25,26] DFT optimization of the 15 initial conformers generated using the Merck Molecular Force Field (MMFF) at various levels of theory (B3LYP/6-31G(d), B97D/TZVP PCM/MeCN and CAM-B3LYP/TZVP PCM/MeCN) resulted in 1, 3 and 5 low-energy DFT conformers (≥1%), respectively. In the lowest-energy CAM-B3LYP/TZVP PCM/MeCN conformer (63.6% population), the C-8 methoxycarbonyl group adopted axial orientation, while the C-9 hydroxy group was axial and formed

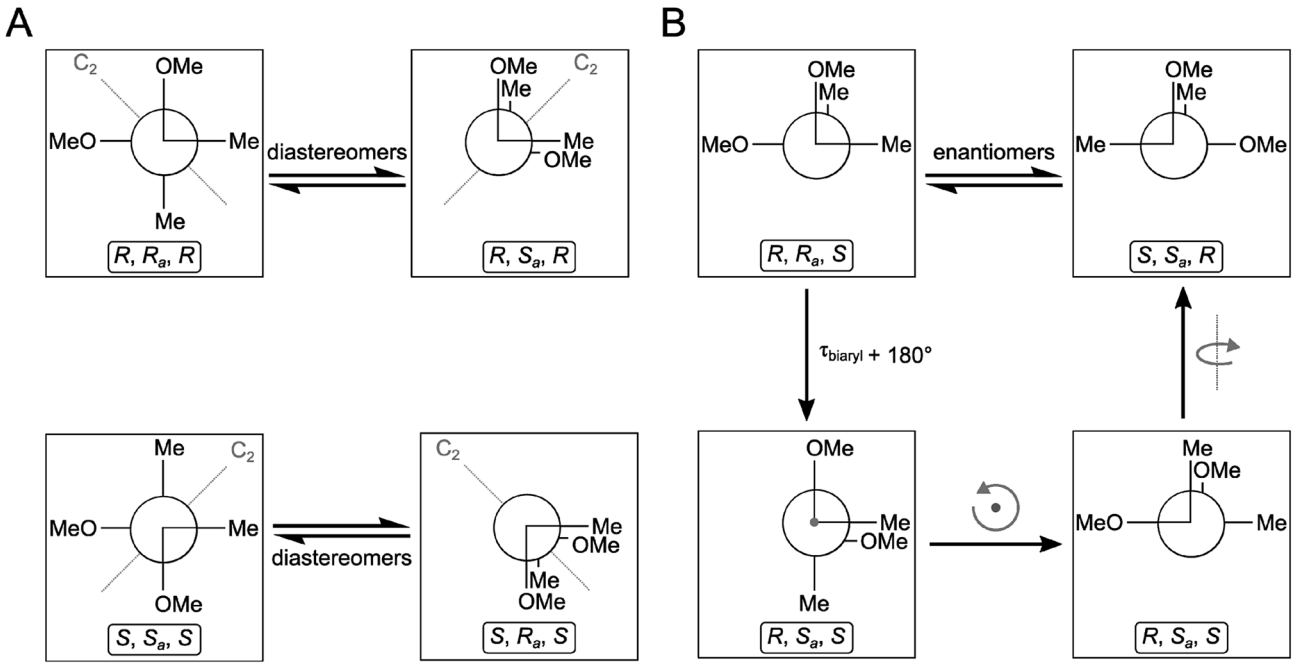

Fig. 3 Stereochemical relationship of atropisomers in the case of the symmetric molecules **2** and **3**. If both molecule halves are homomorph (A), diastereomeric atropisomers result. If both molecule halves are enantiomorph (B), enantiomeric atropisomers result. "Me" and "OMe" relate to C-14 and 15 as well as C-14′ and 15′ in Fig. 1. The grey arrows in the right panel indicate whole-body rotations; the configuration descriptors relate to the central/axial/central chirality elements in the molecules.

Table 6 NMR data of compound **5**[a]

Position	δ_C,[b] type	δ_H (J in Hz)
2	170.9, C	
3	109.6, CH	6.36, s
4	184.4, C	
4a	113.1, C	
5	n.d.[c]	
5a	n.d.	
6	168.6, CH	
8	81.8, CH	6.04, br s
9	70.9, CH	4.92, br s
9a	125.6, C	
10	103.6, CH	7.38, s
10a	158.1, C	
11	170.6, C	
12	20.3, CH_3	2.51, s
OMe-11	52.4, CH_3	3.73, s

[a] Measured in acetone-d_6 (^{1}H at 750 MHz and ^{13}C at 175 MHz). [b] Data were extracted from the HSQC and HMBC spectra. [c] n.d. = not detected.

an intramolecular hydrogen bond to the carbonyl oxygen. Conformers B–D represented geometries with inversed helicity of the α-pyrone ring having equatorial methoxycarbonyl and equatorial hydroxy groups with a total population of 31.4%. Boltzmann-weighted ECD spectra computed for all the sets of conformers of *cis*-(8*R*,9*S*) at various levels (B3LYP/TZVP, BH&HLYP, CAM-B3LYP and PBE0/TZVP) gave a mismatch with the experimental ECD spectrum (Fig. 4). This suggested that the small $^3J_{H\text{-}8,H\text{-}9}$ coupling constant may derive from a *trans*-diequatorial orientation of H-8 and H-9 of the *trans* relative configuration, which, considering the *trans*-diaxial orientation of the large substituents, is less common for 1,2-disubstituted benzene-condensed heterocyclic derivatives. However, we have demonstrated recently by ECD and NMR calculation and X-ray analysis that in benzene-condensed chiral heterocycles the large substituents of contiguous chirality centers preferably adopt *trans*-diaxial orientation both in solution and in the solid-state rendering the protons to *trans*-diequatorial position.[27,28] The same computational ECD protocol was carried out for the arbitrarily chosen *trans*-(8*S*,9*S*) stereoisomer, for which all combinations of the applied levels gave

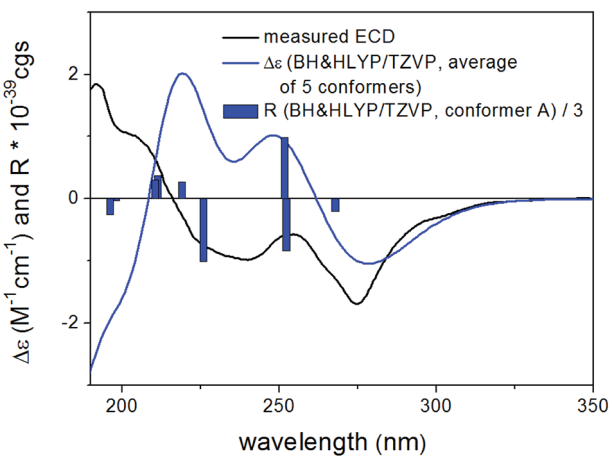

Fig. 4 Experimental ECD spectrum of **5** in MeCN compared with the Boltzmann-weighted BH&HLYP/TZVP PCM/MeCN//CAM-B3LYP/TZVP PCM/MeCN spectrum of the *cis*-(8*R*,9*S*)-**5**.

moderate to good agreement with the experimental ECD spectrum. The diequatorial orientation of the methoxycarbonyl and hydroxy groups was found in conformers A and D with a total population of 46%, while the diaxial geometry was found in conformers B–D and G totaling 53% population. Conformers A and B with opposite helicity of the condensed α-pyrone ring had markedly different computed ECD spectra as demonstrated by their rotatory strengths (Fig. 5). Based on the good ECD agreement, (−)-*trans*-(8*S*,9*S*) absolute configuration was determined for dihydrolateropyrone (**5**).

The five known cryptic compounds that were isolated from the co-culture extracts but were not detected in extracts of the axenic fungal control included lateropyrone (**6**),[24] zearalenone (**7**),[29] (−)-citreoisocoumarin (**8**),[30,31] macrocarpon C (**9**),[5] and 7-hydroxy-2-(2-hydroxypropyl)-5-methylchromone (**10**).[32] In addition, four constitutively present compounds (also detected in axenic fungal controls) including enniatins B, B1 and A1 (**11–13**)[6] and fusaristatin A (**14**)[33] were upregulated in the co-culture extracts.

The new dimeric naphthoquinones **1–4** and the likewise new compound **5** were evaluated for their antibacterial activity against human pathogenic bacterial strains, including *Staphylococcus aureus* and *Pseudomonas aeruginosa* but exhibited no antibacterial activity. For compound **5**, this is in sharp contrast to the structurally closely related known compound lateropyrone (**6**), which had previously been noted for its pronounced activity against Gram positive bacteria.[5] Apparently, hydrogenation of the double bond at C-8 and 9 leads to a complete loss of antibacterial activity.

The observed upregulation of antibiotically active lateropyrone (**6**) and enniatins (**11–13**) during co-cultivation of *F. tricinctum* and *S. lividans* (Table 1) may be interpreted as chemical defense of the fungus.[5] The most interesting finding from this study is, however, the observation that *F. tricinctum* responds to the presence of *S. lividans* in a metabolically different way compared to co-cultures of this fungus with *B. subtilis*, leading to the accumulation of the new compounds **1–4** that are not detected when the fungus is co-cultured with *B. subtilis*. This result mirrors data from a similar study with the fungus *Chaetomium* sp. Co-culture of *Chaetomium* sp. either with *B. subtilis* or with *P. aeruginosa* likewise provoked accumulation of different sets of cryptic fungal compounds.[9,10] Future experiments should aim at unravelling the molecular patterns that underlie these specific fungal metabolic responses.

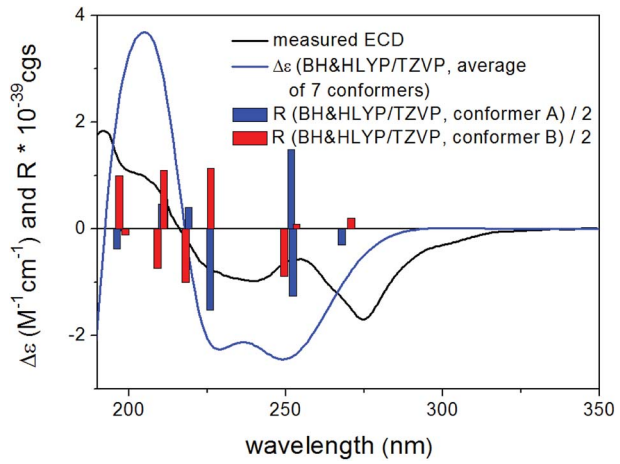

Fig. 5 Experimental ECD spectrum of **5** in MeCN compared with the Boltzmann-weighted BH&HLYP/TZVP PCM/MeCN//CAM-B3LYP/TZVP PCM/MeCN spectrum of the *trans*-(8*S*,9*S*)-**5**.

Experimental section

General experimental procedures

For measuring the optical rotations a Perkin-Elmer-241 MC polarimeter was used. ECD spectra were recorded on a J-810 spectropolarimeter. Solvents used for spectroscopic measurements had spectral grade and for other usage solvents were distilled prior to use. For 1D and 2D NMR spectra, Bruker AVANCE DMX 600 or Bruker ARX 700 NMR spectrometers were used. Mass spectra were recorded with a Finnigan LCQ Deca mass spectrometer, while HRMSESI spectra were acquired with a FTHRMS-Orbitrap (Thermo-Finnigan) mass spectrometer. HPLC chromatograms were obtained with a Dionex P580 system connected to a photodiode array detector (UVD340S). Routine UV lengths for detection were set at 235, 254, 280, and 340 nm. The stationary phase of the analytical column (125 × 4 mm) was Eurosphere-10 C_{18} (Knauer, Germany). The mobile phase was a gradient of acidic nanopure water, set to pH 2 by adding HCOOH and HPLC grade methanol, following the gradient: 0 min, 10% MeOH; 5–35 min, 10–100% MeOH; 35–45 min, 100% MeOH. Semi-preparative HPLC chromatography was performed using the Lachrom–Merck Hitachi semi-preparative HPLC system (UV detector L-7400; pump L-7100; Eurosphere-100 C_{18}, 300 × 8 mm, Knauer, Germany) at a flow rate of 5.0 mL min^{-1}. Column chromatography was carried out using Sephadex LH-20 and Merck MN Silica gel 60 M (0.04–0.063 mm). During the isolation work, precoated silica gel 60 F254 TLC plates (Merck, Darmstadt, Germany) served to control the progress of isolation, under detection at 254 and 365 nm and then sprayed with anisaldehyde reagent.

Microbial material

The endophytic fungus *F. tricinctum* was obtained from healthy fresh rhizomes of *A. paucinervis* (Aristolochiaceae) adapting standard procedures.[34] The fresh plant was collected in January 2006 from the mountains Beni-Mellal, located in Morocco.[6] The bacterial strain *Streptomyces lividans* TK24 (ref. 35) complies to standard laboratory strains.[36]

Identification of fungal material

The fungal microorganism was identified as *F. tricinctum* using the ITS method according to the protocol of molecular biology, by DNA isolation and amplification of the ITS region as previously described.[6] The same strain of the fungus, encoded as F.t., is kept under laboratorial conditions at −80 °C in the Institute of Pharmaceutical Biology and Biotechnology, Heinrich-Heine University, Düsseldorf, Germany.

Co-cultivation of *F. tricinctum* with *S. lividans*

In order to cultivate the fungus and the bacterium under sterile conditions, ten Erlenmeyer flasks (1 L each) were prefilled with solid rice medium (50 g of milk rice, *Oryza*) and Yeast Malt (YM) medium (60 mL), and then autoclaved. Four Erlenmeyer flasks were inoculated with only fungus or bacterium, serving as axenic control cultures. *S. lividans* was precultured using YM medium, which was incubated at 30 °C and shaken at 200 rpm, left overnight to reach exponential mid growth. Since the distribution of the bacterial colonies was not measurable by OD because of agglomeration, the average amount of colonies was estimated visually in order to divide equal amounts of the bacterium to each flask. This has been performed by using a sterilized 5 mL Eppendorf pipette. The bacteria were then added to flasks containing the solid rice medium and left for three days at 30 °C before the fungus was added to the flasks and left at room temperature. This protocol was chosen as the fungus readily killed the bacteria when added simultaneously to the culture flasks. The axenic fungal or bacterial cultures on solid rice media were kept under identical conditions. All flasks were then cultivated at room temperature. Flasks were extracted when the fungus had completely covered the surface of the culture media.

Extraction and isolation

After fermentation, 300 mL EtOAc were added to the fully grown cultures which were then extracted for 8 h under continuous shaking. The EtOAc extracts of the co-cultures of *F. tricinctum* and *S. lividans* following HPLC chromatography were combined, yielding an amount of 3.8 g. This extract was dissolved in a solvent mixture of MeOH–H_2O (9 : 1) followed by partitioning against *n*-hexane. The aqueous MeOH extract was subjected to a Sephadex LH-20 column, using acetone as mobile phase, to obtain 12 fractions (Fr.1–14). The second and third fractions (Fr.2 and 3) were combined due to their similar HPLC profiles followed by separation on a silica column. From the first fraction of this chromatographic separation which was eluted with CH_2Cl_2–MeOH (99 : 1), compound **3** (2.3 mg) was purified using semi-preparative RP-HPLC with 100% MeOH. Fr.4 was further fractionated using a Sephadex LH-20 column with MeOH as mobile phase which yielded compound **1** (10.8 mg) as the subfraction Fr.4–4. Fraction Fr.4–3 was subjected to semi-preparative RP-HPLC to afford compound **4** (2.1 mg). From Fr.5, compounds **5** (0.8 mg), **6** (3.9 mg) and **7** (1.5 mg) were obtained by semi-preparative RP-HPLC with MeOH/H_2O as mobile phase. Compounds **2** and **8** were isolated from Fr.8 by semi-preparative RP-HPLC, where **2** (4.2 mg) was eluted at 100% MeOH and **8** (1.1 mg) at 55% MeOH–H_2O. Furthermore, purification of Fr.10 with semi-preparative HPLC yielded compound **9** (1.1 mg) at 40% MeOH–H_2O and compound **10** (1.2 mg) at 55% MeOH–H_2O elution system.

Fusatricinone A (1). Red solid; $[\alpha]_D^{23}$ 0 (*c* 0.1, DCM); UV (MeOH) λ_{max} 223, 278 and 320 nm; ^{1}H and ^{13}C NMR data see Table 2; HRESIMS $[M + H]^+$ *m*/*z* 653.1141 (calcd for $C_{31}H_{25}O_{16}$ 653.1137).

Fusatricinone B (2). Red solid; $[\alpha]_D^{23}$ 0 (*c* 0.1, DCM); UV (MeOH) λ_{max} 223, 277 and 320 nm; ^{1}H and ^{13}C NMR data see Table 3; HRESIMS $[M + H]^+$ *m*/*z* 639.0977 (calcd for $C_{30}H_{23}O_{16}$, 639.0981).

Fusatricinone C (3). Red solid; $[\alpha]_D^{23}$ 0 (*c* 0.1, DCM); UV (MeOH) λ_{max} 222, 277 and 319 nm; ^{1}H and ^{13}C NMR data see Table 4; HRESIMS $[M + H]^+$ *m*/*z* 667.1289 (calcd for $C_{32}H_{27}O_{16}$, 667.1294).

Fusatricinone D (4). Red solid; $[\alpha]_D^{23}$ 0 (*c* 0.1, DCM); UV (MeOH) λ_{max} 223, 278 and 313 nm; ^{1}H and ^{13}C NMR data see Table 5; HRESIMS $[M + H]^+$ *m*/*z* 667.1299 (calcd for $C_{32}H_{27}O_{16}$, 667.1294).

Dihydrolateropyrone (5). Yellow, amorphous powder; $[\alpha]_D^{23}$ −84 (*c* 0.1, EtOH); UV (MeOH) λ_{max} 229, 243, 263 and 350 nm; ECD (MeCN, λ [nm] ($\Delta\varepsilon$), $c = 0.23$ mM): 399 br (−0.09), 301 (−0.30), 275 (−1.74), 239 (−1.01), 202 sh (1.11), 192 (2.25). ^{1}H and ^{13}C NMR data see Table 6; HRESIMS $[M + H]^+$ *m*/*z* 321.0604 (calcd for $C_{15}H_{13}O_8$, 321.0605).

Calculation of the rotation barrier for compounds 1–4

To obtain an energy profile for the rotation about the central biaryl bond in compounds **1–4** at reasonable computational expense, 8,8′-dihydroxy-3,3′-dimethoxy-2,2′-binaphthyl-1,1′,4,4′-tetrone (Fig. 2B) was used as model compound. First, structures in which the torsion angle defined by atoms C4–C3–C3′-C4′ (Fig. 1) was varied from −180° to 180° in increments of 8° were constructed in the Maestro GUI of the Schrödinger Suite of programs. A single structure with a torsion angle of 0° was added to the resulting series of conformer structures. For each of the resulting 47 structures, a conformational search with a harmonic restraint of 10^4 kcal mol^{-1} rad^{-2} on the corresponding value of the torsion angle was performed using MacroModel and its default settings except for the truncated Newton conjugate gradient method for energy minimization. The minimum energy conformers for each of the 47 searches were then geometry optimized while freezing the respective value of the torsion angle. Geometry optimization was carried out in the gas phase at the B3LYP/6-31G(d) level using the GAUSSIAN 09 software.

Conformational analysis and TDDFT-ECD calculations of 5

Mixed torsional/low-frequency mode conformational searches were carried out by means of the MacroModel 10.8.011 software by using the Merck Molecular Force Field (MMFF) with an implicit solvent model for $CHCl_3$.[37] Geometry reoptimizations were carried out at the B3LYP/6-31G(d) level *in vacuo*, the B97D/TZVP[38,39] and the CAM-B3LYP/TZVP[40] levels with the PCM solvent model for MeCN. TDDFT-ECD calculations were run with various functionals (B3LYP, BH&HLYP, CAM-B3LYP, and PBE0) and the TZVP basis set as implemented in the Gaussian 09 package with the same or no solvent model as in the preceding DFT optimization step.[41] Electronic circular dichroism spectra were generated as sums of Gaussians with 2700 and 3300 cm^{-1} widths at half-height, using dipole-velocity-computed rotational strength values.[42] Boltzmann distributions were estimated from the ZPVE-corrected B3LYP/6-31G(d)

energies in the gas-phase calculations and from the B97D and CAM-B3LYP energies in the solvated ones. The MOLEKEL software package was used for visualization of the results.[43]

Antibacterial assay

The antibacterial activity was determined by using the micro-dilution method in alignment with the CLSI guidelines.[44] Compounds were prepared using a DMSO stock solution with the highest concentration of 0.64% (64 μg mL^{-1}). This was subjected to a prepared inoculum, in which the direct colony suspension method was applied by using an inoculum of 5 × 105 colony forming units per mL. Simultaneously, antibiotics were serial 2-fold diluted in DMSO with the compounds.

Conflicts of interest

There are no conflicts to declare.

Acknowledgements

Financial support by the DFG (GRK 2158) to H. G., R. K. and P. P. is gratefully acknowledged. P. P. also wants to thank the Manchot Foundation for support. H. G. is grateful for computational support and infrastructure provided by the "Zentrum für Informations-und Medientechnologie" (ZIM) at the Heinrich Heine University Düsseldorf and the computing time provided by the John von Neumann Institute for Computing (NIC) on the supercomputer JURECA at Jülich Supercomputing Centre (JSC) (user ID: HKF7). T. K. and A. M. thank the National Research, Development and Innovation Office (NKFI K120181 and PD121020) for financial support and the Governmental Information-Technology Development Agency (KIFÜ) for CPU time.

References

1 A. Marmann, A. H. Aly, W. Lin, B. Wang and P. Proksch, *Mar. Drugs*, 2014, **12**, 1043–1065.
2 G. Daletos, W. Ebrahim, E. Ancheeva, M. El-Neketi, W. Lin and P. Proksch, in *Chemical Biology of Natural Products*, ed. D. Newman, G. Cragg and P. Grothaus, CRC Press, Boca Raton, 2017, ch. 8, pp. 233–284.
3 C. F. Pérez Hemphill, P. Sureechatchaiyan, M. U. Kassack, R. S. Orfali, W. Lin, G. Daletos and P. Proksch, *J. Antibiot.*, 2017, **70**, 726–732.
4 J. Wang, A. Debbab, C. F. Pérez Hemphill and P. Proksch, *Z. Naturforsch.*, 2013, **68c**, 223–230.
5 A. R. B. Ola, D. Thomy, D. Lai, H. Brötz-Oesterhelt and P. Proksch, *J. Nat. Prod.*, 2013, **76**, 2094–2099.
6 W. Wätjen, A. Debbab, A. Hohlfeld, Y. Chovolou, A. Kampkötter, R. A. Edrada, R. Ebel, A. Hakiki, M. Mosaddak, F. Totzke, M. H. G. Kubbutat and P. Proksch, *Mol. Nutr. Food Res.*, 2009, **53**, 431–440.
7 C. G. Shin, D. G. An, H. H. Song and C. Lee, *J. Antibiot.*, 2009, **62**, 687–690.
8 S. Fraeyman, S. Croubels, M. Devreese and G. Antonissen, *Toxins*, 2017, **9**, 228.
9 E. Ancheeva, L. Küppers, S. H. Akone, W. Ebrahim, Z. Liu, A. Mándi, T. Kurtán, W. Lin, R. Orfali, N. Rehberg, R. Kalscheuer, G. Daletos and P. Proksch, *Eur. J. Org. Chem.*, 2017, 3256–3264.
10 S. H. Akone, A. Mándi, T. Kurtán, R. Hartmann, W. Lin, G. Daletos and P. Proksch, *Tetrahedron*, 2016, **72**, 6340–6347.
11 M. Gulshan, G. Y. Zhao, Z. F. Dong and M. Ghopur, *Shengwu Jishu*, 2009, **19**, 43–46.
12 H. Meschke, S. Walter and H. Schrempf, *Environ. Microbiol.*, 2012, **14**, 940–952.
13 R. P. Mellado, *World J. Microbiol. Biotechnol.*, 2011, **27**, 2231–2237.
14 H. Laatsch, *Z. Naturforsch.*, 1990, **45b**, 393–400.
15 H. Laatsch, *Liebigs Ann. Chem.*, 1983, 1886–1900.
16 S. R. LaPlante, P. J. Edwards, L. D. Fader, A. Jakalian and O. Hucke, *ChemMedChem*, 2011, **6**, 505–513.
17 M. Öki, *Top. Stereochem.*, 1983, **14**, 1–63.
18 I. Alkorta, J. Elguero, C. Roussel, N. Vanthuyne and P. Piras, *Adv. Heterocycl. Chem.*, 2012, **105**, 1–188.
19 D. Rönsberg, A. Debbab, A. Mándi, V. Vasylyeva, P. Böhler, B. Stork, L. Engelke, A. Hamacher, R. Sawadogo, M. Diederich, V. Wray, W. Lin, M. U. Kassack, C. Janiak, S. Scheu, S. Wesselborg, T. Kurtán, A. H. Aly and P. Proksch, *J. Org. Chem.*, 2013, **78**, 12409–12425.
20 G. Wu, G. Yu, T. Kurtán, A. Mándi, J. Peng, X. Mo, M. Liu, H. Li, X. Sun, J. Li, T. Zhu, Q. Gu and D. Li, *J. Nat. Prod.*, 2015, **78**, 2691–2698.
21 G. Höfle and K. Röser, *J. Chem. Soc., Chem. Commun.*, 1978, 611–612.
22 R. C. Durley, J. MacMillan and T. J. Simpson, *J. Chem. Soc., Perkin Trans. 1*, 1975, 163–169.
23 I. M. Romaine and G. A. Sulikowski, *Tetrahedron Lett.*, 2015, **56**, 3617–3619.
24 G. W. Bushnell, Y. L. Li and G. A. Poulton, *Can. J. Chem.*, 1984, **62**, 2101–2106.
25 G. Pescitelli and T. Bruhn, *Chirality*, 2016, **28**, 466–474.
26 A. Mándi, I. W. Mudianta, T. Kurtán and M. J. Garson, *J. Nat. Prod.*, 2015, **78**, 2051–2056.
27 P. Zhang, L. H. Meng, A. Mándi, T. Kurtán, X. M. Li, Y. Liu, X. Li, C. S. Li and B. G. Wang, *Eur. J. Org. Chem.*, 2014, 4029–4036.
28 Y. M. Ren, C. Q. Ke, A. Mándi, T. Kurtán, C. Tang, S. Yao and Y. Ye, *Tetrahedron*, 2017, **73**, 3213–3219.
29 W. H. Urry, H. L. Wehrmeister, E. B. Hodge and P. H. Hidy, *Tetrahedron Lett.*, 1966, **27**, 3109–3114.
30 S. Lai, Y. Shizuri, S. Yamamura, K. Kawai and H. Furukawa, *Heterocycles*, 1991, **32**, 297–305.
31 A. Watanabe, Y. Ono, I. Fujii, U. Sankawa, M. E. Mayorga, W. E. Timberlake and Y. Ebizuka, *Tetrahedron Lett.*, 1998, **39**, 7733–7736.
32 J. Xu, J. Kjer, J. Sendker, V. Wray, H. Guan, R. Edrada, W. Lin, J. Wu and P. Proksch, *J. Nat. Prod.*, 2009, **72**, 662–665.
33 Y. Shiono, M. Tsuchinari, K. Shimanuki, T. Miyajima, T. Murayama, T. Koseki, H. Laatsch, T. Funakoshi, K. Takanami and K. Suzuki, *J. Antibiot.*, 2007, **60**, 309–316.

34 J. Kjer, A. Debbab, A. H. Aly and P. Proksch, *Nat. Protoc.*, 2010, **5**, 479–490.
35 H. Chen, G. Daletos, M. S. Abdel-Aziz, D. Thomy, H. Dai, H. Brötz-Oesterhelt, W. H. Lin and P. Proksch, *Phytochem. Lett.*, 2015, **12**, 35–41.
36 D. A. Hopwood, T. Kieser, H. M. Wright and M. J. Bibb, *J. Gen. Microbiol.*, 1983, **129**, 2257–2269.
37 *MacroModel*, Schrödinger, LLC, 2015, http://www.schrodinger.com/MacroModel.
38 S. Grimme, *J. Comput. Chem.*, 2006, **27**, 1787–1799.
39 P. Sun, D. X. Xu, A. Mándi, T. Kurtán, T. J. Li, B. Schulz and W. Zhang, *J. Org. Chem.*, 2013, **78**, 7030–7047.
40 T. Yanai, D. P. Tew and N. C. Handy, *Chem. Phys. Lett.*, 2004, **393**, 51–57.
41 M. J. T. Frisch, G. W. Trucks, H. B. Schlegel, G. E. Scuseria, M. A. Robb, J. R. Cheeseman, G. Scalmani, V. Barone, B. Mennucci, G. A. Petersson, H. Nakatsuji, M. Caricato, X. Li, H. P. Hratchian, A. F. Izmaylov, J. Bloino, G. Zheng, J. L. Sonnenberg, M. Hada, M. Ehara, K. Toyota, R. Fukuda, J. Hasegawa, M. Ishida, T. Nakajima, Y. Honda, O. Kitao, H. Nakai, T. Vreven, J. A. Montgomery Jr, J. E. Peralta, F. Ogliaro, M. Bearpark, J. J. Heyd, E. Brothers, K. N. Kudin, V. N. Staroverov, R. Kobayashi, J. Normand, K. Raghavachari, A. Rendell, J. C. Burant, S. S. Iyengar, J. Tomasi, M. Cossi, N. Rega, J. M. Millam, M. Klene, J. E. Knox, J. B. Cross, V. Bakken, C. Adamo, J. Jaramillo, R. Gomperts, R. E. Stratmann, O. Yazyev, A. J. Austin, R. Cammi, C. Pomelli, J. W. Ochterski, R. L. Martin, K. Morokuma, V. G. Zakrzewski, G. A. Voth, P. Salvador, J. J. Dannenberg, S. Dapprich, A. D. Daniels, Ö. Farkas, J. B. Foresman, J. V. Ortiz, J. Cioslowski and D. J. Fox, *Gaussian 09 (Revision E.01)*, Gaussian, Inc., Wallingford, CT, 2013.
42 P. J. Stephens and N. Harada, *Chirality*, 2010, **22**, 229–233.
43 U. Varetto, *MOLEKEL 5.4*, Swiss National Supercomputing Centre, Manno, Switzerland, 2009.
44 CLSI, *Methods for Dilution Antimicrobial Susceptibility Tests for Bacteria That Grow Aerobically*, Approved Standard Ninth ed. CLSI document M07-A9, Clinical and Laboratory Standards Institute, Wayne, PA, 2012.